Crystal structure and X-ray powder diffraction data for ruxolitinib

Chunguang Dai,[1,2] Yuanjiang Pan,[1] and Xiurong Hu [1,a)]
[1]Department of Chemistry, Zhejiang University, Hangzhou 310027, PR China
[2]Zhejiang Ausun Pharmaceutical Co., Ltd, Taizhou 307016, PR China

(Received 29 September 2022; accepted 20 November 2022)

X-ray powder diffraction data, unit-cell parameters, and space group for ruxolitinib are reported [$a = 8.7211(5)$ Å, $b = 19.6157(15)$ Å, $c = 18.9645(10)$ Å, $\beta = 90.903(6)°$, unit-cell volume $V = 3243.85$ Å^3, $Z = 8$, and space group $P2_1$]. All measured lines were indexed and are consistent with the corresponding space group. No detectable impurities were observed. The single-crystal data of ruxolitinib are also reported [space group $P2_1$, $a = 8.7110(2)$ Å, $b = 19.5857(4)$ Å, $c = 18.9372(4)$ Å, $\beta = 90.8570(10)°$, unit-cell volume $V = 3230.53(10)$ Å^3, $Z = 8$]. The experimental powder diffraction pattern has been well matched with the simulated pattern derived from the single-crystal data.

[doi:10.1017/S0885715622000604]

Key words: X-ray powder diffraction data, ruxolitinib, crystal structure

I. INTRODUCTION

Ruxolitinib, (3R)-3-cyclopenty-3-[4-(7H-pyrrolo[2,3-d] pyrinidin-4-yl)pyrazole-1-yl]propanentrile, has the chemical formula $C_{17}H_{18}N_6$ and is an oral inhibitor of JAK1 and JAK2, which is approved for the treatment of intermediate- and high-risk myelofibrosis (MF) and high-risk polycythemia vera (PV). Ruxolitinib selectively inhibits the proliferation of JAK2-driven Ba/F3 cells and these effects are correlated with decreased levels of phosphorylated JAK2 and of signal transducer and activator of transcription 5 (STAT5) (Plosker, 2015; Lussana et al., 2018). Thus, in November 2011, the U.S. FDA approved ruxolitinib for the treatment of patients with intermediate or high-risk myelofibrosis. On May 24, 2019, ruxolitinib was approved by FAD for steroid-refractory acute graft-versus-host disease (GVHD) in adult and pediatric patients 12 years and older. The chemical structure of ruxolitinib is shown in Figure 1 and its salts, such as ruxolitinib phosphate, hydrochloride, sulfate, besylate, and their polymorphism forms were reported (Albrecht and Selig, 2016; Bernal-Vazquez et al., 2016; Tieger et al., 2017). But the free form of ruxolitinib has not been reported yet. The crystal structures of ruxolitinib and its salts have also not been found yet.

We have not found this compound in the CSD database (Groom et al., 2016) or in the PDF4+ database (Gates-Rector and Blanton, 2019). Therefore, we have decided to characterize this compound by X-ray powder diffraction and X-ray single-crystal diffraction techniques. In our study, we present powder data for ruxolitinib.

II. EXPERIMENTAL

A. Sample preparations

The sample was supplied by Zhejiang Ausun Pharmaceutical Co., LTD (purity >99.9%) and used without further purification. Dissolving ruxolitinib (500 mg) in the mixture of ethyl acetate and butyl acetate (10 ml 1:1 v/v) at reflux temperature and slow cooling of the solutions yielded crystals of ruxolitinib. Then, the crystals were dried, smashed, screened through 50 μm mesh size, and mounted on a flat zero-background plate.

B. Powder diffraction data collection

X-ray powder diffraction data was measured on a SmartLab diffractometer with fixed divergence slits and a D/tex Ultra 250 detector at room temperature. The diffractometer was configured in parafocusing Bragg-Brentano geometry. Data were collected over a 2-θ range of 5° to 50° with a step size of 0.02° and a counting time of 1.0 s/step using a Cu$K\alpha$ radiation at a powder of 40 kV and 180 mA. Cu$K\beta$ radiation was removed using a divergent beam Ni filter. The software package MDI-Jade version 7.5 (Materials Data Inc.,

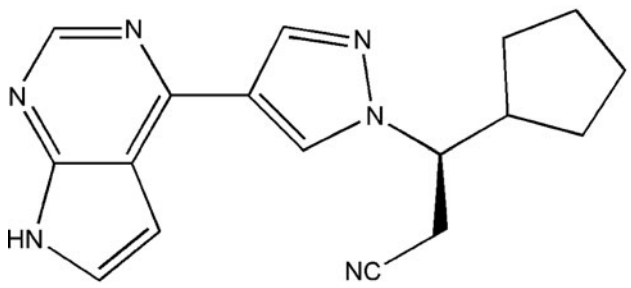

Figure 1. Chemical structure of ruxolitinib.

a)Author to whom correspondence should be addressed. Electronic mail: huxiurong@zju.edu.cn

TABLE I. X-ray powder diffraction data of ruxolitinib.

$2\theta_{obs}$ (°)	d_{obs} (Å)	$(I/I_o)_{obs}$	h	k	l	$2\theta_{cal}$ (°)	d_{cal} (Å)	$\Delta 2\theta$ (°)
6.474	13.6421	1.8	0	1	1	6.478	13.6335	0.004
9.002	9.8154	2.7	0	2	0	9.009	9.8078	0.007
9.320	9.4808	26.4	0	0	2	9.320	9.4811	0.000
10.118	8.7348	16.2	1	0	0	10.136	8.7200	0.017
10.349	8.5411	0.4	0	1	2	10.354	8.5363	0.006
11.078	7.9805	40.4	−1	0	1	11.092	7.9703	0.014
11.977	7.3829	1.0	−1	1	1	11.976	7.3840	−0.002
12.097	7.3102	1.8	1	1	1	12.100	7.3084	0.003
12.973	6.8186	4.5	0	2	2	12.976	6.8167	0.004
13.676	6.4695	46.6	−1	0	2	13.677	6.4692	0.001
13.888	6.3713	53.4	1	0	2	13.894	6.3684	0.007
14.397	6.1470	37.7	−1	1	2	14.405	6.1437	0.008
14.600	6.0622	12.4	1	1	2	14.612	6.0571	0.012
16.439	5.3878	35.4	0	3	2	16.455	5.3827	0.016
17.519	5.0581	44.1	−1	3	1	17.529	5.0551	0.010
17.761	4.9897	9.5	−1	1	3	17.771	4.9870	0.010
18.020	4.9187	34.8	1	1	3	18.024	4.9176	0.004
18.698	4.7417	36.3	0	0	4	18.703	4.7405	0.004
19.244	4.6084	78.5	0	1	4	19.246	4.6079	0.002
19.441	4.5622	16.6	1	3	2	19.441	4.5621	0.001
19.517	4.5445	18.8	0	3	3	19.517	4.5445	0.000
20.348	4.3608	41.0	2	0	0	20.352	4.3600	0.004
20.760	4.2751	13.0	1	4	0	20.764	4.2744	0.004
21.307	4.1666	32.2	−2	1	1	21.308	4.1665	0.000
21.459	4.1375	74.2	1	0	4	21.458	4.1376	0.000
21.658	4.0999	100.0	−1	1	4	21.657	4.1001	−0.001
21.939	4.0480	19.2	1	1	4	21.936	4.0485	−0.003
22.561	3.9377	76.5	2	0	2	22.561	3.9377	0.000
22.750	3.9054	38.9	−2	1	2	22.751	3.9054	0.000
22.852	3.8883	36.9	2	2	1	22.856	3.8877	0.003
23.054	3.8547	10.3	−1	2	4	23.051	3.8552	−0.003
23.311	3.8128	2.7	1	2	4	23.314	3.8122	0.004
23.884	3.7226	5.3	0	1	5	23.878	3.7235	−0.006
24.084	3.6921	1.8	−2	2	2	24.085	3.6920	0.001
24.335	3.6546	5.6	2	2	2	24.338	3.6542	0.002
24.520	3.6274	2.6	2	3	0	24.520	3.6275	−0.001
24.914	3.5710	14.1	−2	3	1	24.910	3.5715	−0.004
25.043	3.5529	18.6	−1	4	3	25.038	3.5535	−0.005
25.140	3.5394	27.6	0	2	5	25.156	3.5372	0.016
25.398	3.5040	36.2	2	1	3	25.387	3.5055	−0.011
25.859	3.4426	11.6	−1	1	5	25.851	3.4437	−0.008
26.146	3.4054	6.8	1	1	5	26.146	3.4054	0.000
26.248	3.3924	5.9	−2	2	3	26.247	3.3925	−0.001
26.556	3.3538	4.8	−1	5	2	26.550	3.3545	−0.005
26.727	3.3328	2.1	0	5	3	26.722	3.3333	−0.004
27.343	3.2590	1.2	2	4	0	27.348	3.2584	0.005
27.671	3.2211	1.1	0	6	1	27.665	3.2217	−0.006
27.812	3.2051	1.4	2	4	1	27.813	3.2050	0.001
28.214	3.1604	5.0	0	0	6	28.214	3.1604	0.000
28.587	3.1200	7.0	0	1	6	28.585	3.1201	−0.002
29.056	3.0707	1.4	2	4	2	29.058	3.0704	0.003
29.146	3.0613	1.5	1	6	0	29.148	3.0612	0.001
29.564	3.0190	2.2	1	6	1	29.560	3.0194	−0.004
29.674	3.0081	5.4	0	2	6	29.674	3.0081	0.000
30.254	2.9517	8.6	−1	1	6	30.247	2.9523	−0.007
30.617	2.9175	2.0	−1	6	2	30.614	2.9178	−0.003
30.737	2.9064	3.0	3	0	0	30.735	2.9067	−0.003
31.001	2.8823	2.3	2	4	3	31.000	2.8824	−0.001
31.516	2.8364	2.4	3	1	1	31.517	2.8362	0.002
31.824	2.8096	0.3	2	1	5	31.819	2.8101	−0.006
32.367	2.7637	2.6	−3	1	2	32.369	2.7635	0.002
32.519	2.7511	1.5	3	2	1	32.517	2.7513	−0.002
33.361	2.6836	2.8	0	1	7	33.363	2.6834	0.002
33.924	2.6403	2.4	1	7	1	33.927	2.6401	0.003
33.987	2.6356	1.5	−3	3	1	33.987	2.6356	0.000
34.338	2.6094	8.6	−1	5	5	34.318	2.6109	−0.020

Continued

https://doi.org/10.1017/S0885715622000604 Published online by Cambridge University Press

TABLE I. Continued

$2\theta_{obs}$ (°)	d_{obs} (Å)	$(I/I_o)_{obs}$	h	k	l	$2\theta_{cal}$ (°)	d_{cal} (Å)	$\Delta 2\theta$ (°)
34.802	2.5757	2.7	1	0	7	34.805	2.5755	0.003
35.078	2.5561	0.3	−2	1	6	35.075	2.5562	−0.002
35.725	2.5112	3.0	−1	2	7	35.715	2.5119	−0.010
36.258	2.4755	0.6	−3	1	4	36.257	2.4756	−0.001
36.509	2.4591	3.1	2	2	6	36.514	2.4588	0.005
36.598	2.4533	1.5	1	7	3	36.593	2.4537	−0.005
36.869	2.4359	4.7	3	3	3	36.865	2.4361	−0.004
37.247	2.4120	1.7	0	7	4	37.243	2.4123	−0.005
37.927	2.3704	2.4	0	0	8	37.928	2.3703	0.001
38.607	2.3301	3.5	−1	7	4	38.613	2.3298	0.006
39.110	2.3013	4.1	−2	1	7	39.109	2.3014	−0.001
39.238	2.2941	2.4	−1	8	2	39.261	2.2928	0.023
39.523	2.2782	3.1	1	0	8	39.523	2.2782	0.001
39.620	2.2729	2.7	0	6	6	39.631	2.2722	0.011
40.497	2.2257	1.1	2	2	7	40.504	2.2253	0.008
41.340	2.1822	1.1	3	5	3	41.349	2.1818	0.009
41.692	2.1646	1.1	0	9	1	41.678	2.1653	−0.014
42.038	2.1476	2.8	4	1	1	42.011	2.1489	−0.026
42.962	2.1035	3.2	2	7	4	42.959	2.1036	−0.003
43.734	2.0681	3.7	4	3	0	43.735	2.0681	0.001
43.818	2.0643	3.2	−1	9	2	43.794	2.0654	−0.025
44.310	2.0426	1.6	−1	7	6	44.289	2.0435	−0.021
44.409	2.0382	4.6	4	1	3	44.373	2.0398	−0.036
45.071	2.0098	4.3	−2	7	5	45.072	2.0098	0.001
45.162	2.0060	4.7	2	6	6	45.168	2.0057	0.006
45.819	1.9788	2.1	4	4	1	45.833	1.9782	0.014
46.364	1.9567	3.3	4	3	3	46.360	1.9569	−0.004

USA) was used to smooth the data, fit the background, strip off the $K\alpha_2$ component and obtain the peak positions and intensities (Table I). The $K\alpha_1$ (λ = 1.5406 Å) wavelength was used in converting observed 2-θ to d-spacing.

C. Single-crystal diffraction data collection

X-ray single-crystal diffraction data were collected at 296(2) K with a Bruker D8 Venture diffractometer with Cu$K\alpha$ radiation (λ = 1.54178 Å) for cell determination and subsequent data collection. Data reduction was performed by APEX3 software and multi-scan absorption correction was applied. Using Olex2 (Dolomanov et al., 2009), the structure was solved with the ShelXT (Sheldrick, 2015a) structure solution program using intrinsic phasing and refined with the ShelXL (Sheldrick, 2015b) refinement package using Least Squares minimization.

III. RESULTS AND DISCUSSION

Indexing of the experimental X-ray diffraction patterns and unit-cell refinements was done using MDI-Jade (Materials Data Inc., 2002). The cell refinement results which were combined with the results of single-crystal diffraction and characteristics of a chiral molecule, showed that ruxolitinib belonged to monoclinic with space group $P2_1$ and unit-cell parameters: a = 8.7211(5) Å, b = 19.6157(15) Å, c = 18.9645(10) Å, β = 90.903(6)°, unit-cell volume V = 3243.85 Å^3, Z = 8, ρ = 1.2546 g/cm^3. The figure of merit is F_{30} = 203.9(0.0059,30) (Smith and Snyder, 1979). The values of $2\theta_{obs}$, d_{obs}, I_{obs}, h, k, l, $2\theta_{cal}$, d_{cal}, and $\Delta 2\theta$ are listed in Table I.

The single-crystal experiment was carried out at the temperature of 296 K and the structure solution was obtained (space group $P2_1$, a = 8.7110(2) Å, b = 19.5857(4) Å, c = 18.9372(4) Å, β = 90.8570(10)°, unit-cell volume V = 3230.53(10) Å^3, Z = 8, ρ = 1.260 g/cm^3). The detailed single-crystal data and the experimental data are summarized in Table II. The figures were drawn with ORTEP-3 (Oak

TABLE II. Crystal and experimental data of ruxolitinib.

Emperical formula	$C_{17}H_{18}N_6$
Formula weight	306.37
Temperature (K)	296(2)
Crystal system	Monoclinic
Space group	$P2_1$
a (Å)	8.7110(2)
b (Å)	19.5857(4)
c (Å)	18.9372(4)
β (°)	90.8570(10)
Volume (Å^3)	3230.53(12)
Z	8
ρ (g/cm^3)	1.260
μ (mm^{-1})	0.638
F(000)	1296
Radiation	Cu$K\alpha$ (λ = 1.54178 Å)
2-θ range for data collection (°)	3.25−68.23
Index ranges	$-10 \le h \le 10$, $-23 \le k \le 23$, $-22 \le l \le 22$
Reflections collected	44,067
Independent reflections	10,907
Data/restraints/parameters	10,907/1/829
Goodness of fit on F^2	1.020
Final R indexes [$I \ge 2\sigma(I)$]	$R1$ = 0.0442, w$R2$ = 0.1208
Final R indexes (all data)	$R1$ = 0.0473, w$R2$ = 0.1245
Largest diffraction peak/hole (e/Å^3)	0.459/−0.257

https://doi.org/10.1017/S0885715622000604 Published online by Cambridge University Press

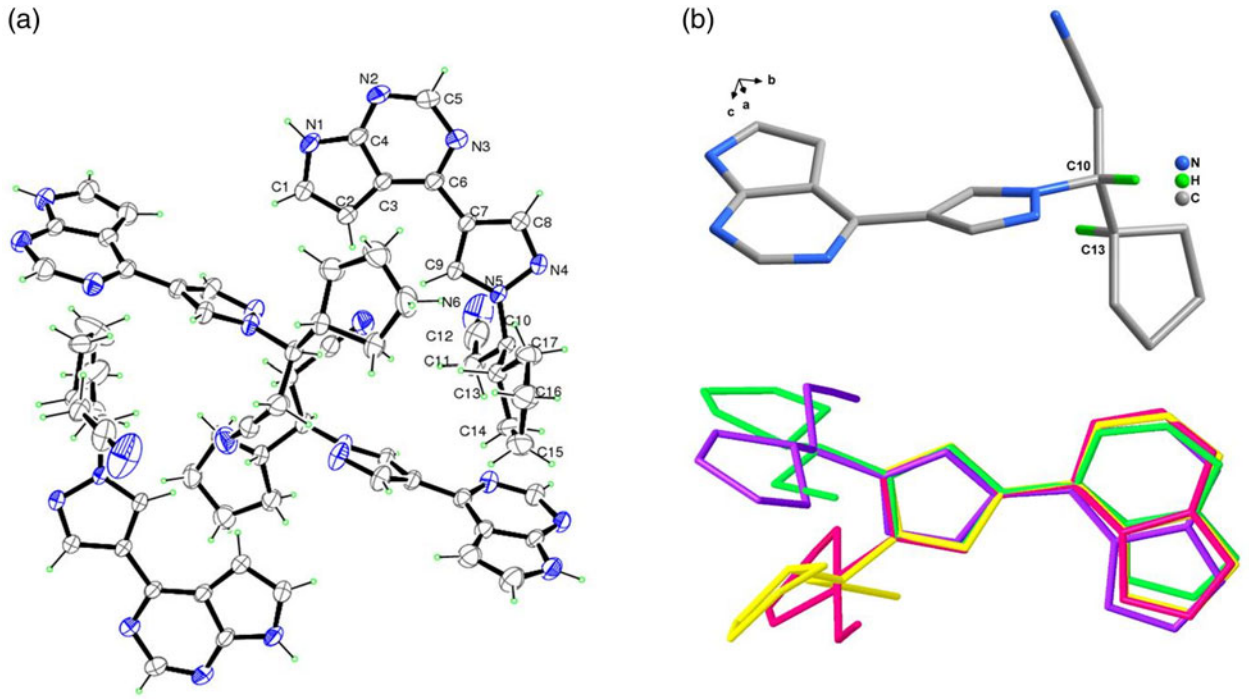

Figure 2. (a) Asymmetric unit of ruxolitinib shown in thermal ellipsoid model with 30% probability. (b) Overlay of configurations for four ruxolitinib molecules.

Ridge Thermal Ellipsoid Plot) and Diamond (Brandenburg and Putz, 2005). The asymmetric units of the title compound contain four ruxolitinib molecules, which have slightly different conformations, and mainly shows the different orientation of pyrazole-1-yl]propanentrile. Meanwhile, the groups of 7H-pyrrolo[2,3-d]pyrinidin in four molecules are dislocated slightly each other, which are revealed from torsion angles of C9–C7–C6–N3, C3–C6–C7–C9 and their correspondings. But the configurations of chiral C atoms (C10, C10A, C10B, C10C) of four ruxolitinib molecules in the asymmetric unit are the same "R" configuration (Figure 2). Intermolecular hydrogen bond interactions N–H···N and other weak intermolecular interactions link ruxolitinib molecules, forming two-dimensional layer packing along *bc*-directions.

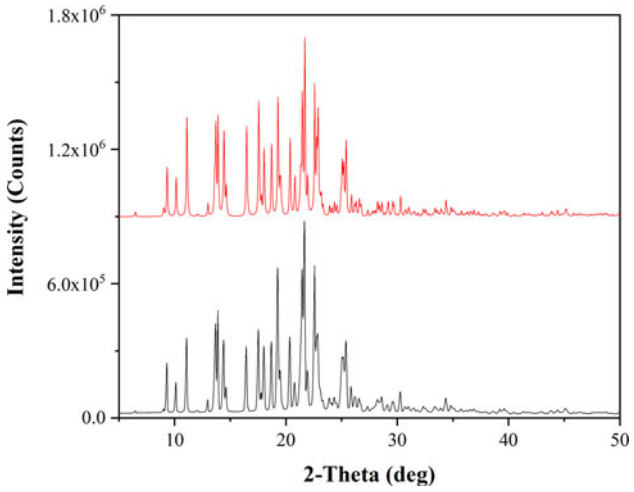

Figure 3. X-ray powder diffraction pattern (black line) and the simulated pattern of the crystal structure (red line) of ruxolitinib.

The comparison of the experimental powder diffraction pattern and the simulated pattern derived from the single-crystal data is shown in Figure 3. Results showed that both single-crystal and powder diffraction methods can get the similar structure data and the deviations of the unit-cell parameters and unit-cell volume were between 0.05 and 0.41%.

IV. DEPOSITED DATA

The Crystallographic Information Framework (CIF) file was deposited with the ICDD. The data can be requested at pdj@icdd.com.

FUNDING

This work was financially supported from Zhejiang University Experimental Technology Research (SYBJS202204).

REFERENCES

Albrecht, W., & R. Selig. 2016. "Salts of (R)-3-(4-(7H-pyrrolo[2,3-D] pyrimidin-4-yl)-LH-pyrazole-L-yl)-3-Cyclopentylpropanenitrile with Benzenesulfonic Acid," the Patent Corporate Body Aruga Patent Office WO2016026975A.

Bernal-Vazquez, P. M., J. M. Lazcano-Seres, J. A. Juarez-Lagunas, M. D. L. A. Cano-Herrera, D. K. M. Van, A. Cedillo-Cruz, & R. J. M. Mendoza. 2016. "Solid Form of Ruxolitinib," the Patent Corporate Body Aruga Patent Office CA2928286A.

Brandenburg, K., & H. Putz. 2005. *Diamond-Crystal and Molecular Structure Visualization*. Bonn, Germany, Crystal Impact GbR.

Dolomanov, O. V., L. J. Bourhis, R. J. Gildea, J. A. K. Howard, and H. Puschmann. 2009. "OLEX2: A Complete Structure Solution, Refinement and Analysis Program." *Journal of Applied Crystallography* 42: 339–41.

https://doi.org/10.1017/S0885715622000604 Published online by Cambridge University Press

Gates-Rector, S., and T. Blanton. 2019. "The Powder Diffraction File: A Quality Materials Characterization Database." *Powder Diffraction* 34: 352–60.

Groom, C. R., I. J. Bruno, M. P. Lightfoot, and S. C. Ward. 2016. "The Cambridge Structural Database." *Acta Crystallographica Section B: Structural Science, Crystal Engineering and Materials* 72: 171–9.

Lussana, F., M. Cattaneo, A. Rambaldi, and A. Squizzato. 2018. "Ruxolitinib-Associated Infections: A Systematic Review and Meta-Analysis." *American Journal of Hematology* 93: 339–47.

Materials Data Inc. (MDI). 2002. *Jade 7.5 XRD Pattern Processing Software*. Livermore, CA, USA, Materials Data.

Plosker, G. L. 2015. "Ruxolitinib: A Review of Its Use in Patients with Myelofibrosis." *Drugs* 75: 297–308.

Sheldrick, G. M. 2015a. "SHELXT - Integrated Space-Group and Crystal-Structure Determination." *Acta Crystallographica. Section A, Foundations and Advances* A71: 3–8.

Sheldrick, G. M. 2015b. "Crystal Structure Refinement with SHELXL." *Acta Crystallographica. Section A, Foundations and Advances* C71: 3–8.

Smith, G. S., and R. L. Snyder. 1979. "F_N: A Criterion for Rating Powder Diffraction Patterns and Evaluating the Reliability of Powder-Pattern Indexing." *Journal of Applied Crystallography* 12: 60–5.

Tieger, E., H. Tozickova, M. Tkadlecova, O. Dammer, & T. Gurgut. 2017. "Crystalline Forms of (3R)-3-cyclopentyl-3-[4-(7H-pyrrolo[2,3-D]pyrimidin-4-yl)-pyrazol-L-yl]-Propanenitrile Salts and Preparation Thereof," the Patent Corporate Body Aruga Patent Office WO2017125097A.

https://doi.org/10.1017/S0885715622000604 Published online by Cambridge University Press